

Accuracy assessment of rainfall prediction by global models during the landfall of tropical cyclones in the North Indian Ocean

Swati Bhomia, Neeru Jaiswal* and C. M. Kishtawal

Atmospheric Sciences Division, AOSG, EPSA, Space Applications Centre (ISRO), Ahmedabad, India

ABSTRACT: The rainfall prediction accuracy of seven state-of-the-art operational models during landfall (LF) of tropical cyclones formed in the North Indian Ocean was assessed. The rainfall predicted by these models 1–3 days (24–72 h) before the LF day of tropical cyclones was compared with TRMM_3B42 rainfall data. Cyclone induced rainfall occurs along its track; thus rainfall within 600 km along the cyclone track was used for comparison. The error in cyclone track prediction affects the rainfall prediction. This has been taken care of by shifting the rainfall distribution over the cyclone best track positions provided by the India Meteorological Department. The validation statistics for the rainfall prediction accuracy of the models were computed by combining the forecasts generated by these seven models during LF of nine cyclones formed in the North Indian Ocean during 2010–2013. The skill of the models was analysed using different rainfall validation measures/statistics. Based on these validation statistics it was found that, of the seven global models, the models from four centres, namely the National Center for Environment Prediction, the European Centre for Medium-range Weather Forecasts, the UK Meteorological Office and the Canadian Meteorological Centre, performed closer to the observations. However, there was no single model which was able to exhibit all the features of the observed rainfall.

KEY WORDS tropical cyclone; rainfall; TRMM_3B42; TIGGE; landfall; accuracy assessment

Received 10 May 2015; Revised 7 September 2016; Accepted 23 November 2016

1. Introduction

Tropical cyclones (TCs) are devastating natural hazards associated with strong winds, heavy rains and storm surges. The Indian sub-continent is among the worst cyclone affected regions of the world, with a coast line of 7516 km (5400 km along the mainland, 132 km in Lakshadweep and 1900 km in Andaman and Nicobar Islands), exposed to nearly 5–7% of the world's TCs (Singh *et al.*, 2001; Oouchi *et al.*, 2006). TCs in the North Indian Ocean (NIO) occur in the months of April–June and October–December, with a primary peak in November and secondary peak in May, which affect the coastal regions of India, Bangladesh, Myanmar, Sri Lanka, Oman and Pakistan. These TCs account for a large number of deaths, loss of livelihood opportunities, loss of public and private properties and severe damage to infrastructure. Broad scale assessment of the population at risk suggests that an estimated 320 million people are vulnerable to TC related hazards in India (Peduzzi *et al.*, 2012). Climate change and its resultant impact on TC frequency and intensity (Kishtawal *et al.*, 2012; Mendelsohn *et al.*, 2012) and sea level rise (Nicholls and Cazenave, 2010) can significantly increase the vulnerability of the coastal population. Torrential rainfall (more than 30 cm h^{-1}) associated with TCs is a major cause of damage. Heavy rainfall from a cyclone is usually spread over a wide area and causes large scale soil erosion and weakening of embankments. Heavy and prolonged rains due to cyclones may cause flash floods, river floods and submergence of low lying areas causing loss of life and property. Floods and

coastal inundation due to storm surges pollute drinking water sources causing outbreaks of epidemics. It has been reported that almost 60% of the deaths related to TCs in the United States were due to flash floods caused by heavy rainfall (Rappaport, 2000). The accurate prediction of total rainfall amount and its distribution during landfall (LF) of TCs is crucial for planning and mitigation of TC related disaster.

The distribution of rainfall patterns during TCs depends on various factors, i.e. the internal dynamics of the cyclone and environmental characteristics. The cyclone translational speed has a significant impact on the azimuthal asymmetries of the rainfall and the total rainfall duration at a location as slow moving systems are more likely to stay at one location than fast moving systems (Shapiro, 1983). It has been reported in the literature that vertical wind shear creates asymmetries in the inner-core field rainfall distribution pattern (Bender, 1997; Jones, 2000; Frank and Ritchie, 2001; Black *et al.*, 2002; Corbosiero and Molinari, 2002; Rogers *et al.*, 2003; Lonfat *et al.*, 2004). The intensity of the storm, the environmental humidity and the properties of the underlying surface can impact the amount and distribution of rainfall received from a landfalling TC (Marchok *et al.*, 2007). These factors have been incorporated in numerical weather prediction (NWP) models using different parameterization schemes. With the advancement of computational resources and developments in model physics, NWP models have become highly sophisticated and accurate in providing forecasts of various meteorological parameters at high spatial and temporal scales. It has been reported that the accuracy of forecasts in track prediction of TCs by NWP models has been significantly improved in the last two decades whereas the accuracy of intensity prediction has not improved much (Franklin *et al.*, 2003; DeMaria *et al.*, 2005). However, there have been very few studies that focused on the validation and improvement of rainfall forecasts. Evaluation of the precipitation accuracy of the Geophysical

* Correspondence: N. Jaiswal, Atmospheric Sciences Division, Atmospheric and Oceanic Sciences Group (AOSG), EPSA, Space Applications Centre (ISRO), Ahmedabad-380015, Gujarat, India. E-mail: neerujaiswal@gmail.com

Table 1. Summary of the seven models validated in the study obtained from the TIGGE archive.

Centre	Resolution	Forecast length (day)	Forecasts per day ^a
CMA	0.56° × 0.56°	10	2
CMC	0.9° × 0.9°	16	2
ECMWF	N200 (reduced Gaussian) N128 after day 10	15	2
UKMO	0.83° × 0.55°	15	2
NCEP	1.00° × 1.00°	16	4
KMA	1.00° × 1.00°	10	2
CPTEC	0.94° × 0.94°	15	2

^aA single deterministic forecast generated at 0000 UTC was used in the study.

Fluid Dynamics Laboratory model for TCs forming in the North Atlantic basin and affecting the US coast has been discussed by DeMaria and Tuleya (2001). The different validation schemes for TC rainfall prediction have been discussed by Marchok *et al.* (2007). However, no work has been carried out so far to assess the rainfall prediction accuracy of models during landfall of TCs in the NIO. In order to improve rainfall prediction by the models, their validation and intercomparison using observations (*in situ* or satellite) is required. This accuracy assessment of the models will help in understanding the limitations of different models. The THORPEX Interactive Grand Global Ensemble (TIGGE) dataset which includes forecasts from the global NWP models from different forecast centres provides an opportunity to intercompare their prediction accuracy.

In the present study, rainfall predicted by the global models during LF of TCs in the NIO was examined. The rainfall prediction accuracy of the models was assessed for 24, 48 and 72 h lead time before LF of the cyclones with respect to TRMM_3B42 rainfall data using different rainfall validation statistics, namely total volumetric rain, pattern correlation, equitable threat score (ETS) and root mean square error (RMSE). The radial distribution of the rainfall pattern within cyclones of different sizes and intensities is also discussed.

2. Data used

The TIGGE dataset provides a forecast of all basic meteorological variables from the leading operational global forecast centres, namely the National Center for Environment Prediction (NCEP), the European Centre for Medium-range Weather Forecasts (ECMWF), the UK Meteorological Office (UKMO), the Canadian Meteorological Centre (CMC), the China Meteorological Administration (CMA), the Japan Meteorological Agency, the Korea Meteorological Administration (KMA), the Australian

Bureau of Meteorology, the Météo-France and the Brazilian Centra de Previsao de Tempo e Estudos Climatico (CPTEC), with different forecast lengths (4–16 days) in real time (Richardson, 2005). This dataset is available to researchers with a 2 day latency and has been used in TC track forecasting (Majumdar and Finocchio, 2010; Yamaguchi and Majumdar, 2010).

The data used in the present study were obtained from the ECMWF portal of the TIGGE dataset which can be accessed from the website <http://apps.ecmwf.int/datasets/data/tigge>. There is an online facility of grid customization of data before download, which includes the grid resolution and the region of interest. This online facility provides data at a lower or higher resolution than that at which they were produced as *per* the requirement. Data that were originally archived on different grids for different models were bilinearly interpolated to the new grid.

Seven global models that provide forecasts with a larger lead time (greater than 5 days), i.e. CMA, CMC, ECMWF, NCEP, UKMO, KMA and CPTEC, were used in this work for validation of rainfall prediction during the LF of TCs. A summary of these models is given in Table 1. Each model in the TIGGE database provides ensemble based probabilistic forecasts and single deterministic forecasts. In the present study, a single deterministic forecast from each model during the LF of TCs was used. In the TIGGE portal, data are available with different resolutions and grid schemes for different models. The resolution of data and domain of analysis have some impact on validation statistics (Tustison *et al.*, 2001; Gallus, 2002). Since all the models used in this study provide forecasts at different grid resolutions, forecasts from all these models were interpolated to 0.25° × 0.25° using an online interpolation scheme provided by the ECMWF TIGGE portal.

The rainfall forecasts generated by the seven models during the LF of nine TCs formed during the period 2010–2013 in the NIO region were analysed for rainfall accuracy assessment. A summary of these cyclones is given in Table 2. The cyclones were of different intensities and sizes and affected different coastal regions of the Indian subcontinent. The forecasts of three meteorological parameters, i.e. total precipitation, surface winds (horizontal and meridional winds at 10 m) and mean sea level pressure (MSLP), generated by the seven models, at 0000 UTC on LF day (T0), 24 h before LF day (T0-24), 48 h before LF day (T0-48) and 72 h before LF day (T0-72), of the above nine cyclones were obtained from the ECMWF TIGGE portal. The wind and MSLP data were used to locate cyclones in the model predicted fields. The forecasts generated at a similar time (0000 UTC), which were available for all seven models and nine cyclones at the TIGGE portal, were used in this work.

Three hourly TRMM_3B42 data of rainfall during the nine cyclones were obtained through the internet (<ftp://trmmopen.gsfc.nasa.gov/pub/merged>) and were used as observations. The

Table 2. Summary of the cyclones formed during 2010–2013 in the North Indian Ocean.

Cyclone name	Life duration	Maximum intensity (kn)	Landfall day (T0) and time	Intensity during landfall (kn)
VIYARU	10–16 May 2013	45	16 May 06 Z	45
PHAILIN	9–12 October 2013	115	12 October 15 Z	115
HELEN	19–22 November 2013	55	22 November 06 Z	55
LEHAR	23–28 November 2013	75	28 November 06 Z	30
MADI	6–12 December 2013	65	12 December 12 Z	25
NILAM	28–31 October 2012	45	31 October 09 Z	45
THANE	25–30 December 2011	75	30 December 00 Z	75
LAILA	17–21 May 2010	55	20 May 09 Z	55
JAL	4–7 November 2010	60	7 November 15 Z	30

observed track of cyclone intensity, LF position and time were taken from the best track provided by the India Meteorological Department (IMD).

3. Methodology

Rainfall prediction provided by the seven global models during LF of nine NIO cyclones was analysed to assess their prediction skill. For each of the nine cyclones, the rainfall predicted by the seven global models at 0000 UTC of days T0-24, T0-48 and T0-72 was compared with observed rainfall using different statistical measures. All nine cyclones decayed within 12–24 h after their LF. To make the time domain homogeneous, forecasts up to 12 h after LF were included in the study.

Since rainfall occurs along the cyclone track, it is important to identify the position of the cyclone in different forecast steps of the models. For identification of TCs in the different forecast steps, a wind pattern matching approach was used. In this approach a synthetic cyclone is generated and its wind circulation pattern is matched with the wind field in the study region. The synthetic cyclone was constructed using the functional relationship provided by Chan and Williams (1987):

$$V(r) = V_m \left(\frac{r}{R_m} \right) \exp \left[\frac{1}{b} \left\{ 1 - \left(\frac{r}{R_m} \right)^b \right\} \right] \quad (1)$$

where V is the tangential velocity at radius r , V_m is the maximum value of the tangential velocity, R_m is the radius at which V_m occurs and b is a shape parameter. This synthetic vortex was used to identify the cyclone in the model forecasts. The wind pattern matching was done by computing the matching index between the wind vectors (u and v at 10 m height) of the above two wind fields. For this, wind vector components were considered as complex variables, e.g. $A = u + iv$. The matching index (c) between the two sets of such complex numbers was computed (Jaiswal *et al.*, 2013) as follows:

$$c = 1 - \frac{(1/N) \sum_{i=1}^N (|A_i - B_i|)^2}{\sqrt{(1/N) \sum_{i=1}^N (|A_i - \bar{A}|)^2} \sqrt{(1/N) \sum_{i=1}^N (|B_i - \bar{B}|)^2}} \quad (2)$$

where \bar{A} and \bar{B} represent the mean value of the complex vectors A , i.e. synthetic cyclone wind fields, and B , i.e. model forecasted wind fields, respectively. N is the dimension of vector A (or B). The matching between the two wind fields yields high values of the matching index ($c > 0.5$) if cyclonic circulations are detected in the forecasts. The MSLP was the other parameter which was used in addition to the wind fields for detecting the existing cyclonic systems. The grid with the highest value of the matching index was considered as the cyclone position. In the next forecast step, the search region for cyclone position was restricted around the previous step position so that the same cyclone would be identified. This method was used to identify the cyclone position at every 6 h forecast step for all forecasts used in this study. The best track data of the cyclones obtained from the IMD were used to determine the cyclone positions in the TRMM_3B42 rainfall data.

Rain due to a TC occurs along the track of the cyclone and the amount of rain decreases over the region farthest from the track. Thus, grids within 600 km of the cyclone track were masked and used for computing the rainfall validation statistics.

The total volume of rainfall is an important parameter as it may cause flooding and water inundation. Thus, the total volumetric rain is computed for assessing the accuracy of the models. For this, the total volumetric rain predicted by each of the models, generated on days T0-24, T0-48 and T0-72, was computed for all nine TCs. The total volumetric rain due to the cyclone was obtained by adding the value of the rain volume at pixels within the 600 km of track of the TCs. The amount of volumetric rain at each pixel was computed by multiplying the area of the pixel ($\sim 25 \times 25 \text{ km}^2$) with the rain rate (mm h^{-1}) at that pixel. Forecasts of all cyclones were combined to determine the volumetric rain ($\text{km}^3 \text{ day}^{-1}$) predicted by each individual model on day T0-24, T0-48 and T0-72 separately. The total volumetric rain values for similar days were also computed in the observations using the above steps for computing the validation statistics.

Rainfall during a TC is not distributed evenly over the cyclonic region. The heaviest rainfall occurs in the core of the cyclone which is relatively smaller than the complete cyclone canopy size. Due to asymmetry in the cyclone, there is more rain on one side of the cyclone and less on the other side. The observed rainfall along the best track for all nine cyclones considered in the present study is shown in Figure S1. It is thus important to match the whole distribution pattern of rainfall to validate the accuracy of the models for rainfall prediction during cyclones. To validate the prediction of the whole rainfall distribution pattern over the cyclone by different models, two statistical measures were computed, i.e. the pattern correlation and the ETS. The spatial distribution of rainfall was compared by computing the pattern correlation between the rainfall predicted by the models in forecasts generated at 0000 UTC on days T0-24, T0-48 and T0-72 and observations. These pattern correlations were computed for all seven models by combining rainfall predictions for all nine cyclones. The computations included values of the rainfall within 600 km of the cyclone track position.

The ETS (Tuleya *et al.*, 2007) measures the number of forecast fields that match the observed threshold amount. It is the ratio of the number of forecast hits to the total number of forecast hits and misses, including a chance factor to account for the number of hits that would be expected to occur purely due to random chance. It can be expressed as:

$$\text{ETS} = \frac{H - H_{\text{random}}}{F + O - H - H_{\text{random}}} \quad (3)$$

where H is the number of locations where forecast rainfall amount matches or exceeds the observed rainfall amount for a given rainfall threshold. F and O are the numbers of forecasts and observations, respectively, satisfying the threshold criteria. H_{random} is a random chance that both the forecast and observation meet, which is obtained using:

$$H_{\text{random}} = \frac{FO}{F + O} \quad (4)$$

The ETS was computed for different rainfall thresholds for all seven models using the discussed methodology.

The ETS and the pattern correlations are dependent on the specific geographical location of the forecast and the observed amounts of rainfall and are thus sensitive to model track forecast errors (Marchok *et al.*, 2007). Thus, the rainfall in the forecast field was shifted by the displacement vector error of the cyclone position in forecasts which was computed with respect to the IMD best track positions. To study the effect of cyclone track error, values of pattern correlation and ETS were computed without track shift (WOTS) and with track shift (WTS) (i.e.

Table 3. Comparison of rainfall volume ($\text{km}^3 \text{ day}^{-1}$) predicted by the models at 0000 UTC 72 h before landfall day of the cyclones (T0-72) and observations.

	TRMM_3B42	CMA	CMC	ECMWF	UKMO	NCEP	KMA	CPTEC
Rainfall volume ($\text{km}^3 \text{ day}^{-1}$)	28.68	24.75	26.61	24.33	30.69	27.75	25.44	25.17
Mean rainfall bias ($\text{km}^3 \text{ day}^{-1}$)	–	–3.93	–2.07	–4.35	2.01	–0.93	–3.24	–3.51
Rainfall bias (%)	–	–13.70	–7.22	–15.17	7.01	–3.24	–11.30	–12.24

Table 4. Comparison of rainfall volume ($\text{km}^3 \text{ day}^{-1}$) predicted by the models at 0000 UTC 48 h before landfall day of the cyclones (T0-48) and observations.

	TRMM_3B42	CMA	CMC	ECMWF	UKMO	NCEP	KMA	CPTEC
Rainfall volume ($\text{km}^3 \text{ day}^{-1}$)	25.74	19.71	26.07	22.02	26.7	24.33	25.05	24.42
Mean rainfall bias ($\text{km}^3 \text{ day}^{-1}$)	–	–6.03	0.33	–3.72	0.96	–1.41	–0.69	–1.32
Rainfall bias (%)	–	–23.43	1.28	–14.45	3.73	–5.48	–2.68	–5.13

rainfall field shifted/corrected with respect to the IMD best track). The rainfall distribution during Cyclone Phailin for seven models WOTS and WTS and for observations during LF is shown in Figure S2.

Five out of the nine cyclone cases considered in the present study made LF with intensities greater than 35 kn and affected the coastal area. The distribution pattern of rainfall prediction after LF depends on different land surface model mechanisms used within model physics. To compare the rainfall predicted by the models during LF of the cyclones, the forecasts generated at 0000 UTC on LF day (T0) of these five cyclones, over the land region, were analysed. The histograms of the rainfall in the radial bins along the track of the cyclone over the land were computed and mean rainfall values in each of the radial bins were compared. The values obtained for each of the cyclones were combined to compare the accuracy of model with respect to observations.

4. Results

The rainfall predicted by each of the seven global models for nine TCs in the NIO was individually analysed and combined to evaluate the prediction accuracy of the models. The statistical comparison of the forecasts generated by all the models at 0000 UTC 24 h (T0-24), 48 h (T0-48) and 72 h (T0-72) before LF day (T0) are discussed in this section based on different validation measures.

4.1. Volumetric rainfall

The predicted total volumetric rainfall ($\text{km}^3 \text{ day}^{-1}$) and mean rainfall bias from the seven global models with respect to TRMM_3B42 rainfall for a lead prediction time 72, 48 and 24 h before LF day are summarized in Tables 3–5, respectively. It can be seen from Table 3 that at day T0-72 the total volumetric rain predicted by the NCEP model was $27.75 \text{ km}^3 \text{ day}^{-1}$ which

was close to the observed value ($28.68 \text{ km}^3 \text{ day}^{-1}$) followed by the UKMO model ($30.69 \text{ km}^3 \text{ day}^{-1}$) and the CMC model ($26.61 \text{ km}^3 \text{ day}^{-1}$). For day T0-48 the total volumetric rain predicted by the CMC model ($26.07 \text{ km}^3 \text{ day}^{-1}$) was close to the observed value $25.74 \text{ km}^3 \text{ day}^{-1}$ followed by the KMA model ($25.05 \text{ km}^3 \text{ day}^{-1}$) and UKMO model ($26.70 \text{ km}^3 \text{ day}^{-1}$). The total volumetric rain predicted on day T0-24 by the UKMO model was $23.57 \text{ km}^3 \text{ day}^{-1}$, which was close to the observed rainfall ($23.39 \text{ km}^3 \text{ day}^{-1}$) followed by the KMA model ($24.32 \text{ km}^3 \text{ day}^{-1}$) and the CMC model ($22.29 \text{ km}^3 \text{ day}^{-1}$). Thus, for the longer lead prediction time, the performance of the NCEP model was more skilful than the other models. However, at the early lead prediction time the best performing models were CMC and UKMO. The same was evident from the rainfall bias.

4.2. Pattern correlation

Figures 1(A)–(C) show the pattern correlation between the rainfall predicted by the seven global models and observations on days T0-72, T0-48 and T0-24, respectively. The correlation values are shown for both cases, i.e. WOTS and WTS. It can be seen in Figure 1(A) that, for prediction on day T0-72, the highest value of pattern correlation is found for the NCEP model, i.e. 0.60 WOTS and 0.70 WTS, followed by the ECMWF, CMC and UKMO models. Figure 1(B) shows that, for prediction on day T0-48, the NCEP model has the highest correlation (0.66 WOTS) followed by the CMC, ECMWF and UKMO models, whereas WTS the correlation value of the CMC model was found to be the highest (0.71) followed by the ECMWF, NCEP and UKMO models. Figure 1(C) shows that for prediction on day T0-24 the NCEP model was better than other models as the correlation values obtained were 0.72 WOTS and 0.73 WTS. These results show that track correction improved the rainfall prediction skill. For all three forecasts generated 72, 48 and 24 h before LF day, the NCEP model was found to perform better than the other models.

Table 5. Comparison of rainfall volume ($\text{km}^3 \text{ day}^{-1}$) predicted by the models at 0000 UTC 24 h before landfall day of the cyclones (T0-24) and observations.

	TRMM_3B42	CMA	CMC	ECMWF	UKMO	NCEP	KMA	CPTEC
Rainfall volume ($\text{km}^3 \text{ day}^{-1}$)	23.39	18.72	22.29	19.65	23.57	21.81	24.32	21.44
Mean rainfall bias ($\text{km}^3 \text{ day}^{-1}$)	–	–4.67	–1.10	–3.74	0.18	–1.58	0.93	–1.95
Rainfall bias (%)	–	–19.97	–4.69	–15.98	0.78	–6.74	3.98	–8.34

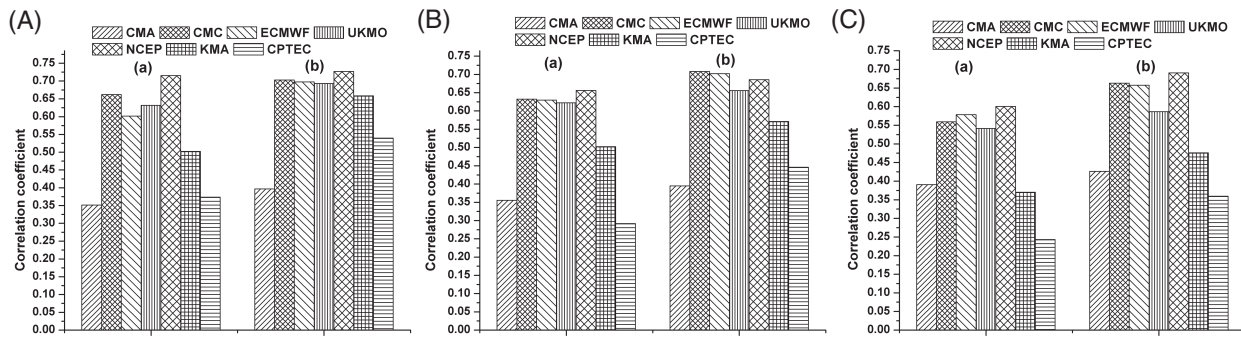


Figure 1. (A) Comparison of the correlation co-efficient between the model predicted rainfall at 0000 UTC on day T0-72 and the observed rainfall during landfall of all nine cyclones along (a) the best track of the India Meteorological Department (IMD) (without track shift, WOTS) and (b) the model predicted track shifted over the best track of the IMD (with track shift, WTS). (B) Comparison of the correlation co-efficient between the model predicted rainfall at 0000 UTC on day T0-48 and the observed rainfall during landfall of all nine cyclones along (a) the best track of the IMD (WOTS) and (b) the model predicted track shifted over the best track of the IMD (WTS). (C) Comparison of the correlation co-efficient between the model predicted rainfall at 0000 UTC on day T0-24 and the observed rainfall during landfall of all nine cyclones along (a) the best track of the IMD (WOTS) and (b) the model predicted track shifted over the best track of the IMD (WTS).

4.3. Equitable threat score (ETS)

The ETS was computed WOTS and WTS for a range of thresholds including low to high rainfall values, namely 0.1–250 mm. The values of the ETS obtained for the rainfall predicted by the seven models on day T0-72 WOTS and WTS are shown in Figures 2(a) and (b), respectively. Figure 2(a) shows that the ETS values for thresholds up to 75 mm are higher for the NCEP model (0.29–0.40) followed by the ECMWF (0.21–0.38) and UKMO (0.21–0.32) models for a rainfall threshold up to 75 mm. At 75 and 100 mm rain thresholds, the values of the ETS for the ECMWF (0.27, 0.23), UKMO (0.26, 0.24) and NCEP (0.27, 0.23) models were almost equal and the other models had lower values. For thresholds greater than 100 mm, the NCEP model was found to have the highest value (0.17) of the ETS followed by the CMC (0.16), UKMO (0.06) and ECMWF (0.02) models. Figure 2(b) shows that after track correction the NCEP model (0.34–0.49) showed the highest values of ETS for almost all the rainfall thresholds. However, at the lower values of rain threshold (30–50 mm) the ETS values of the ECMWF model were slightly better than the NCEP model followed by the UKMO model. At the 100 mm rain threshold the ETS values of the NCEP (0.30) and the CMC (0.30) models were equal followed by the ECMWF (0.26) and UKMO (0.22) models. The ECMWF and UKMO models were the second best models up to 50 mm rainfall threshold. The CMC model had the second highest values of ETS after the NCEP model for a rainfall threshold greater than 50 mm.

The ETS values for rainfall prediction generated on day T0-48 day WOTS and WTS are shown in Figures 3(a) and (b), respectively. It can be seen in Figure 3(a) that the NCEP (0.33–0.40) and ECMWF (0.23–0.29) models have higher ETS values at lower rain thresholds (<75 mm) than the other models. At 75 mm rain threshold the ETS value of the NCEP (0.31), ECMWF (0.30), UKMO (0.30) and CMC (0.31) models were very similar. For higher rain threshold values of 100, 200 and 250 mm, the NCEP model shows higher values of ETS (0.30, 0.20 and 0.14) followed by the CMC model (0.25, 0.12 and 0.07) and the UKMO model (0.29, 0.11 and 0.07), respectively. Figure 3(b) shows that after track correction the ETS values of all models were improved at lower rain thresholds. At higher rain thresholds the NCEP model was performing better followed by the ECMWF, UKMO and CMC models.

For rainfall prediction on day T0-24, the ETS values WOTS and WTS are shown in Figures 4(a) and (b), respectively. It can

be seen in Figure 4(a) that the NCEP model (0.06–0.40) showed the highest ETS for rain threshold followed by the ECMWF (0.04–0.38), CMC (0.0–0.34) and UKMO (0.0–0.34) models. After track correction, it can be seen from Figure 4(b) that the spread in ETS for the NCEP (0.10–0.40), ECMWF (0.02–0.41), UKMO (0.0–0.39) and CMC (0.0–0.39) models is improved.

These results show that ETS values computed WOTS and WTS at higher rain thresholds ($>100 \text{ mm day}^{-1}$) are low compared to lower rain thresholds ($0.1–100 \text{ mm day}^{-1}$). One possible reason is the inherent limitation of the ETS formulation. This has the disadvantage that it tends to zero for vanishingly rare events, i.e. higher rain values. This creates the misleading impression that rare events cannot be skilfully forecasted no matter which forecasting system is used (Stephenson *et al.*, 2008). Further, despite the similar techniques used in both hurricane modelling and general circulation models, a difference appears in the relative importance of some of the physical processes and in the horizontal resolution required to resolve the mesoscale nature of the TC. Thus, cumulus convection and latent heating which are often of secondary importance for general circulation models are dominant in TC models (Anthes, 1982). This leads to the inefficiency of global models to resolve the extreme rainfall during TCs, thereby showing a decrement in skill towards the higher rainfall thresholds ($>100 \text{ mm day}^{-1}$).

4.4. Distribution of mean rainfall along the TC track

A comparison of the distribution of mean rainfall along a TC track is a good indicator of the model's capability for predicting the rainfall distribution pattern. The mean rainfall prediction values were computed in 100 km swaths centred over the cyclone track position predicted by each model. Similar computations of mean rainfall distribution were calculated with the observed data using the IMD best track positions. The values of the mean rainfall obtained by each model and observation for swaths 100 km from the cyclone centre are shown in Figure 5. The rainfall decreases beyond the centre of the cyclone. This characteristic of the rainfall distribution is presented by each of the models. Figure 5(a) shows that in the core of the cyclone (within 100 km) the mean observed rainfall is 41.92 mm; however, the ECMWF (71.87 mm) and NCEP (52.45 mm) models overestimate the rainfall and other models underestimate. The estimated rainfall by the NCEP model within the 100–200 km

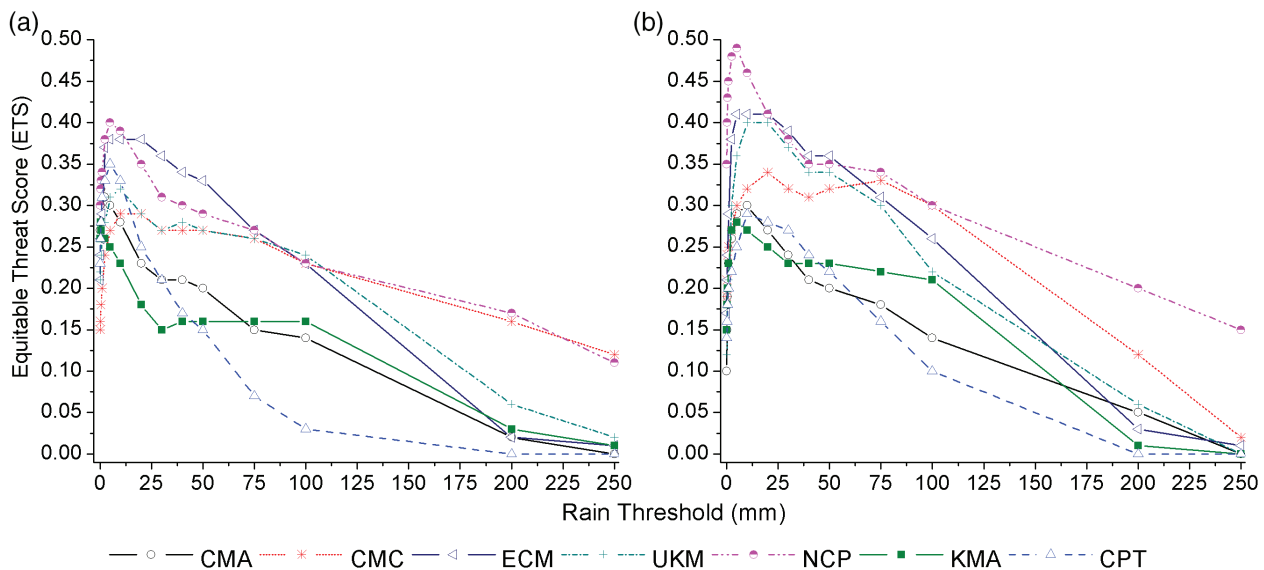


Figure 2. Equitable threat score of rainfall prediction at 0000 UTC on day T0-72 for the nine cyclones for all the models along (a) the India Meteorological Department (IMD) best track positions in the model and (b) the model forecasted rain field shifted over the IMD best track. [Colour figure can be viewed at wileyonlinelibrary.com].

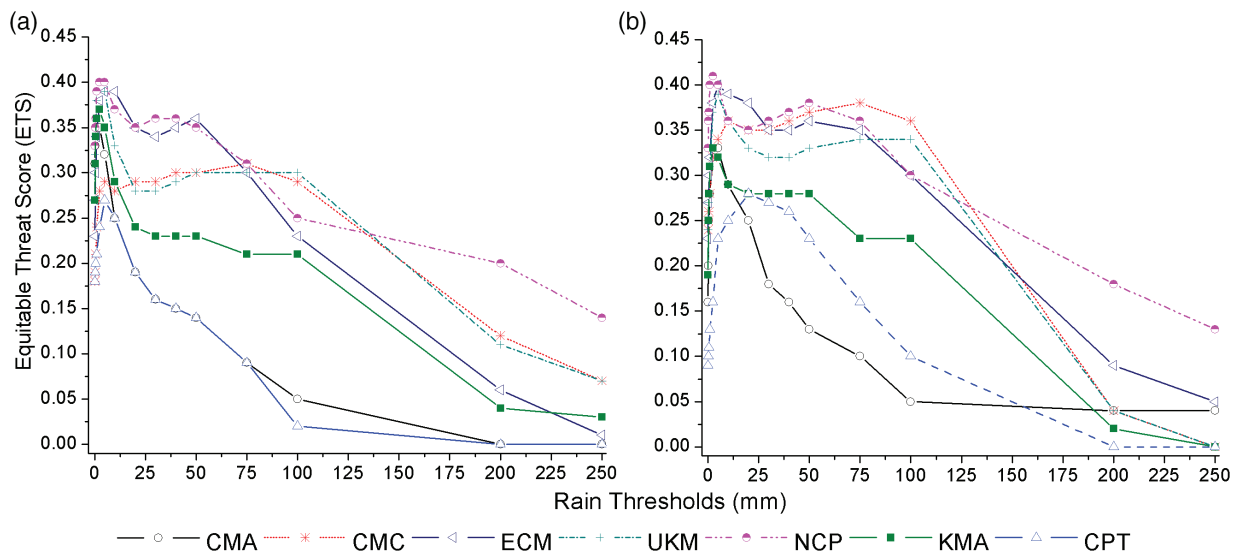


Figure 3. Equitable threat score of rainfall prediction at 0000 UTC on day T0-48 for the nine cyclones for all the models along (a) the India Meteorological Department (IMD) best track positions in the model and (b) the model forecasted rain field shifted over the IMD best track. [Colour figure can be viewed at wileyonlinelibrary.com].

swath from the cyclone was 31.41 mm which is very close to the observed mean rainfall (31.32 mm), followed by the ECMWF model (26.97 mm). After correcting for track error, the radial distribution was again estimated and is shown in Figure 5(b). The values of predicted rainfall are found to be improved after shifting the track. The mean predicted rainfall within 100 km of the TC track by the UKMO, CMC and NCEP models was found to be closer to the observed values than by the other models. Beyond 300 km radial distance from the cyclone centre it was found that all the models were underestimating the mean rainfall amount.

4.5. Root mean square error (RMSE)

The RMSE in the total predicted rainfall during LF was estimated for the forecasts on days T0-24, T0-48 and T0-72, respectively,

with respect to the observations. The RMSE values were also computed after correcting the track positions in the forecasts. The RMSE for both cases WOTS and WTS are shown in Figures 6(a) and (b), respectively, for all seven models. The performance of the models can be ranked based on the values of the RMSE. For forecasts generated on day T0-24 after track correction, the minimum RMSE values are found for the UKMO (20 mm h^{-1}) model followed by the NCEP (26 mm h^{-1}) and ECMWF (27 mm h^{-1}). For rainfall predicted on day T0-48, the minimum RMSE values were found for the NCEP (17 mm h^{-1}) model followed by the UKMO (20 mm h^{-1}) and ECMWF (35 mm h^{-1}). For forecasts generated on day T0-72, the ECMWF (30 mm h^{-1}) model had the minimum RMSE values followed by the CMC (35 mm h^{-1}) and UKMO (37 mm h^{-1}) models. Based on the above analysis, for 24 h before LF prediction day, the UKMO model was found

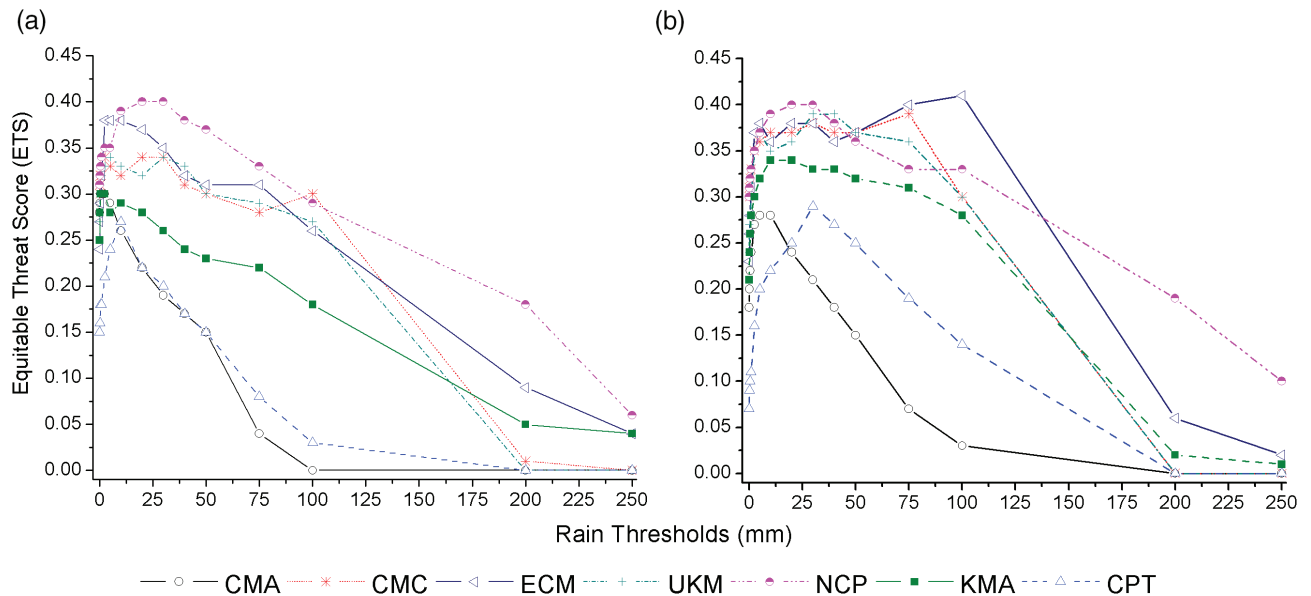


Figure 4. Equitable threat score of rainfall prediction at 0000 UTC on day T0–24 for the nine cyclones for all the models along (a) the India Meteorological Department (IMD) best track positions in the model and (b) the model forecasted rain field shifted over the IMD best track. [Colour figure can be viewed at wileyonlinelibrary.com].

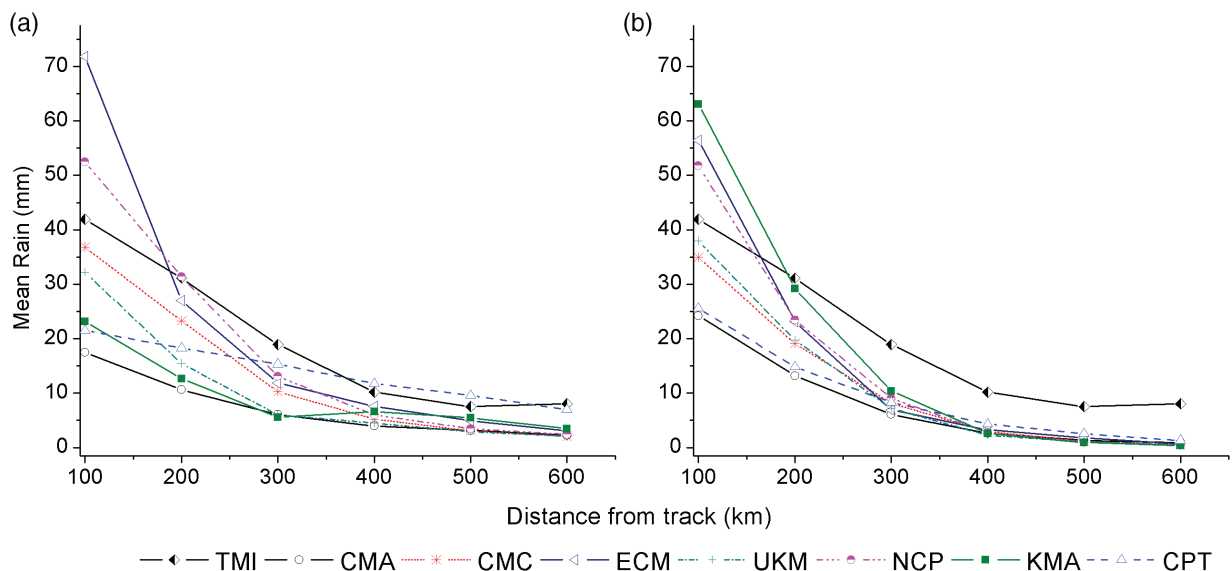


Figure 5. Radial distribution of the mean storm total rainfall, predicted at 0000 UTC on day T0, averaged over all storms in the study for all models and observations as a function of cross-track distance from (a) the India Meteorological Department best track and (b) the model forecasted storm track. [Colour figure can be viewed at wileyonlinelibrary.com].

as the best model for predicting the most accurate rainfall during the LF of TCs followed by the ECMWF and NCEP. For 48 and 72 h before LF of TCs, the best performing models were NCEP and ECMWF, respectively.

4.6. Error spread using boxplots

The error spread in precipitation forecast with respect to observations using boxplots for each model during LF of TCs 24–72 h in advance is presented in Figure S3. In 24 h the forecast improvement after track shift correction is not noticeable because of the fewer track errors in the models, whereas from 24 to 72 h forecasts the track errors in the models increase and hence improvement can be noticed after track shift in the error spread of each

model. The KMA model shows the highest improvement followed by the CPTEC, NCEP, UKMO, ECMWF, CMA and CMC models. With this analysis it was observed that the track error in the KMA model is the highest followed by the CPTEC model compared to the IMD best track.

4.7. Summary of the relative skills of the models using a Taylor diagram

A Taylor diagram was plotted for summarizing the relative skills of the seven models for predicting rainfall during LF of TCs 24, 48 and 72 h ahead of LF day (Figure S4). Figures S4(a)–(f) summarize the relative skill with which the seven global circulation models forecast 1–3 days in advance the spatial pattern of

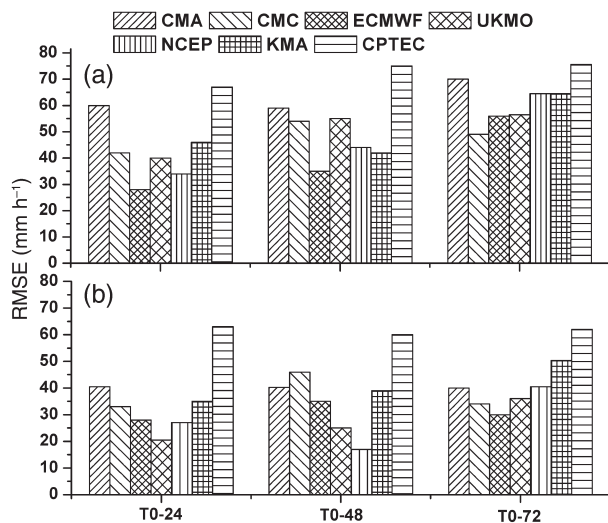


Figure 6. Root mean square error (mm h^{-1}) of storm total rainfall, predicted at 0000 UTC on T0-24, T0-48 and T0-72 h, during landfall of the tropical cyclones in the study for all models (a) without track correction and (b) with track correction.

precipitation during a TC LF. Each model was labelled A–G in the plot to represent the skill. The position of each letter in the plot quantifies how closely the forecast of that model matches observations. For example, it can be seen from Figures S4(a) and (b) that in the 24 h forecast of model C (ECMWF), its pattern correlation with observation is about 0.60 WOTS and 0.72 WTS, respectively. The centred root mean square difference between forecasted and observed patterns is proportional to the distance from the point marked OBS on the x -axis. The contours (centred over the point OBS) indicate the RMSE values and it can be seen that in the case of model C the centred RMSE is about 36 mm day^{-1} WOTS and 31 mm day^{-1} WTS. For model C the standard deviation (SD) (38 mm day^{-1}) of the forecasted field is clearly less than the observed SD (43 mm day^{-1}). The relative merits of the seven models can be inferred from the figures for WOTS and WTS in day T0-24, T0-48 and T0-72 forecasts. The forecasted patterns that agree well with observations will lie nearest to the point marked OBS on the x -axis. Models lying near to this point will have higher correlation and low RMSE. Models lying on the arc joining the point OBS to the y -axis will have the correct SD (which indicates that the pattern variations are of the right amplitude). It can be seen from the figure that the correlation is improved and the RMSE has been reduced for all the models after introducing the track shift correction. This improvement can be seen at all forecast steps. Another inference that can be made is that models B (CMC), C (ECMWF), D (UKMO) and E (NCEP) generally agree best with observations, each with about the same RMSE and correlation. Among the poorly performing models, models A (CMA) and G (CPTEC) have low pattern correlation compared to F (KMA).

5. Conclusions

In the present study, the rainfall prediction accuracy of seven state-of-the-art global models during landfall (LF) of tropical cyclones (TCs) is discussed. The rain predicted by these models for lead prediction times 24, 48 and 72 h before LF of the TCs was compared with the TRMM_3B42 rainfall product using different statistical measures. The analysis of the prediction

skill of individual models suggested that the prediction skill largely differs from model to model both at spatial and temporal scales. The post LF validation statistics show that the NCEP, ECMWF, UKMO and CMC models perform more closely to the observations compared to the rest of the models. Therefore, it can be inferred from the present study that no single model exhibits all the features of the observed rainfall. However, in order to yield more reliable forecasts, rainfall forecasts from these models could be combined using multi-model ensemble techniques in the future. The present analysis showed that the skill towards the extreme rainfall ($>100 \text{ mm day}^{-1}$) values decreases, which may be due to the limitation of the statistical measure (i.e. equitable threat score (ETS)) used. Other verification scores for validating skill for extreme rainfall, in order to overcome the disadvantage of the ETS, namely its vanishing nature towards higher rainfall values, can be explored in future work. In the present study the cyclone track error has been taken into account; however, the impact on rainfall distribution due to cyclone rotation was not included. For further improvement in addition to the track error correction, cyclone rotation can also be taken into consideration in future work.

Acknowledgements

The Director, Space Applications Centre (ISRO), Ahmedabad, is thanked. Acknowledgement goes to the THORPEX Interactive Grand Global Ensemble (TIGGE) (<http://tigge-portal.ecmwf.int>) for providing the valuable model output database, NASA (<ftp://trmmopen.gsfc.nasa.gov/pub/merged>) for providing the TRMM_3B42 product, and the India Meteorological Department (IMD) and the Joint Typhoon Warning Center (JTWC) for providing the best track data of TCs. The anonymous reviewers and the editor are also acknowledged for their valuable comments and suggestions for improving the quality of the paper.

Supporting information

The following material is available as part of the online article:

Figure S1. Track of the nine cyclones overlaid on the total rainfall (mm) observed by the TRMM_3B42 rainfall product within 600 km distance along the track.

Figure S2. Rainfall distribution during landfall of Cyclone Phailin from seven models (with and without track shift corrections) and observations.

Figure S3. Boxplot showing the error spread in 24, 48 and 72 h precipitation forecasts without and with track shift corrections for each model with respect to the observations during landfall of tropical cyclones.

Figure S4. Taylor diagrams displaying a statistical intercomparison of seven model estimates of the rainfall with respect to observations during tropical cyclone landfall without and with track shift corrections.

References

- Anthes RA. 1982. Tropical cyclones their evolution, structure and effects. *Am. Meteorol. Soc.* **19**(41): 208.
- Bender MA. 1997. The effect of relative flow on the asymmetric structure in the interior of hurricanes. *J. Atmos. Sci.* **54**: 703–724.
- Black ML, Gamache JF, Marks FD, Samsury CE, Willoughby HE. 2002. Eastern Pacific Hurricanes Jimana of 1991 and Olivia of 1994: the effect of vertical shear on structure and intensity. *Mon. Weather Rev.* **130**: 2291–2312.

- Chan JCL, Williams RT. 1987. Analytical and numerical studies of the beta-effect in tropical motion. *J. Atmos. Sci.* **44**: 1257–1265.
- Corbosiero KL, Molinari J. 2002. The effects of vertical wind shear on the distribution of convection in tropical cyclones. *Mon. Weather Rev.* **130**: 2110–2123.
- DeMaria M, Mainelli M, Shay LK, Knaff JA, Kaplan J. 2005. Further improvements to the Statistical Hurricane Intensity Prediction Scheme (SHIPS). *Weather Forecasting* **20**: 531–543.
- DeMaria M, Tuleya RE. 2001. Evaluation of quantitative precipitation forecasts from the GFDL hurricane model. *Preprints, Symposium on Precipitation Extremes: Prediction, Impacts, and Responses*, American Meteorological Society, Albuquerque, NM; 340–343.
- Frank WM, Ritchie EA. 2001. Effects of vertical wind shear on the intensity and structure of numerically simulated hurricanes. *Mon. Weather Rev.* **129**: 2249–2269.
- Franklin JL, McAdie CJ, Lawrence MB. 2003. Trends in track forecasting for tropical cyclones threatening the United States, 1970–2001. *Bull. Am. Meteorol. Soc.* **84**: 1197–1203.
- Gallus WA. 2002. Impact of verification grid-box size on warm-season QPF skill measures. *Weather Forecasting* **17**: 1296–1302.
- Jaiswal N, Kishtawal CM, Pal PK. 2013. Prediction of tropical cyclogenesis in North Indian Ocean using Oceansat-2 scatterometer (OSCAT) winds. *Meteorol. Atmos. Phys.* **119**: 137–149. <https://doi.org/10.1007/s00703-012-0230-8>.
- Jones SC. 2000. The evolution of vortices in vertical shear: III: Baroclinic vortices. *Q. J. R. Meteorol. Soc.* **126**: 3161–3185.
- Kishtawal CM, Jaiswal N, Singh R, Niyogi D. 2012. Tropical cyclone intensification trends during satellite era (186–2010). *Geophys. Res. Lett.* **39**: L10810.
- Lonfat M, Marks FD Jr, Chen SS. 2004. Precipitation distribution in tropical cyclones using the Tropical Rainfall Measuring Mission (TRMM) microwave imager: a global perspective. *Mon. Weather Rev.* **132**: 1645–1660.
- Majumdar SJ, Finocchio PM. 2010. On the ability of global ensemble prediction systems to predict tropical cyclone track probabilities. *Weather Forecasting* **25**: 659–680.
- Marchok T, Rogers R, Tuleya R. 2007. Validation schemes for tropical cyclone quantitative precipitation forecasts: evaluation of operational models for U.S. landfalling cases. *Weather Forecasting* **22**: 726–746.
- Mendelsohn R, Emanuel K, Chonabayashi S, Bakkensen L. 2012. Impact of climate change on global tropical cyclone damage. *Nat. Clim. Change* **2**: 205–209.
- Nicholls RJ, Cazenave A. 2010. Sea level rise and its impact on coastal zones. *Science* **328**: 1517–1519.
- Oouchi K, Yoshimura J, Yoshimura H, Mizuta R, Noda A. 2006. Tropical cyclone climatology in global warming climate as simulated in a 20 km mesh global atmospheric model: frequency and wind intensity analysis. *J. Meteorol. Soc. Jpn.* **84**(2): 259–276.
- Peduzzi P, Chatenoux B, Dao H, De Bono A, Herold C, Kossin J, et al. 2012. Global trends in tropical cyclone risk. *Nat. Clim. Change* **2**: 289–294.
- Rappaport EN. 2000. Loss of life in the United States associated with recent Atlantic tropical cyclones. *Bull. Am. Meteorol. Soc.* **81**: 2065–2073.
- Richardson D. 2005. The THORPEX Interactive Grand Global Ensemble (TIGGE). *Geophys. Res. Abstr.* **7**: 02815.
- Rogers RF, Chen SS, Tenerelli JE, Willoughby HE. 2003. A numerical study of the impact of vertical shear on the distribution of rainfall in Hurricane Bonnie (1998). *Mon. Weather Rev.* **131**: 1577–1599.
- Shapiro LJ. 1983. The asymmetric boundary layer flow under a translating hurricane. *J. Atmos. Sci.* **40**: 1984–1998.
- Singh OP, Khan TMA, Rahman MS. 2001. Has the frequency of intense tropical cyclone increased in North Indian Ocean. *Curr. Sci.* **80**: 575–580.
- Stephenson DB, Casati B, Ferro CAT, Wilson CA. 2008. The extreme dependency score: a non-vanishing measure for forecasts of rare events. *Meteorol. Appl.* **15**: 41–50.
- Tuleya RE, Mark D, Kuligowski RJ. 2007. Evaluation of GFDL and simple statistical model rainfall forecasts for U.S. landfalling tropical storms. *Weather Forecasting* **22**: 56–70.
- Tustison B, Harris D, Foufoula-Georgiou E. 2001. Scale issues in verification of precipitation forecasts. *J. Geophys. Res.* **106**: 11 775–11 784.
- Yamaguchi M, Majumdar SJ. 2010. Using TIGGE data to diagnose initial perturbations and their growth for tropical cyclone ensemble forecasts. *Mon. Weather Rev.* **138**: 3634–3655.